Available online at www.sciencedirect.com

ScienceDirect

Procedia Engineering 148 (2016) 1388 – 1395

Procedia Engineering

www.elsevier.com/locate/procedia

4th International Conference on Process Engineering and Advanced Materials

Influence of Lanthanide Promoters on Ni/SBA-15 Catalysts for Syngas Production by Methane Dry Reforming

Osaze Omoregbe[a], Huong T. Danh[b], S.Z. Abidin[a], H.D. Setiabudi[a], Bawadi Abdullah[c], Khanh B. Vu[d], Dai-Viet N. Vo[a,e,*]

[a]*Faculty of Chemical & Natural Resources Engineering, Universiti Malaysia Pahang, Lebuhraya Tun Razak, 26300 Gambang, Kuantan, Pahang, Malaysia*

[b]*Clean Energy and Chemical Engineering, Korea University of Science and Technology (UST), Daejeon, 305-350, Korea*

[c]*Chemical Engineering Department, Universiti Teknologi PETRONAS, 31750, Tronoh, Perak, Malaysia*

[d]*NTT Hi-Tech Institute, Nguyen Tat Thanh University, 298-300A Nguyen Tat Thanh Street, Ho Chi Minh City, Vietnam*

[e]*Centre of Excellence for Advanced Research in Fluid Flow, Universiti Malaysia Pahang, 26300 Gambang, Kuantan, Pahang, Malaysia*

Abstract

The catalytic performance of Ce- and La-promoted Ni/SBA-15 catalysts for syngas production from CO_2 reforming of methane has been investigated in a fixed-bed reactor at stoichiometric feed composition. Both promoted and unpromoted catalysts possessed high BET surface area of 303-445 m^2 g^{-1}. Additionally, SBA-15 support had a relatively uniform rod-like shape with a diameter of about 0.55 µm and a reduction in the crystallite size of NiO phase from 27.0 to 19.1 nm was observed with promoter addition reasonably due to the strong interaction between promoter and NiO particles. CeO_2 and La_2O_3 dopants were finely dispersed on catalyst surface. Temperature-programmed oxidation of spent catalysts showed that coke-resistance was improved significantly with promoter modification and 3%La-10%Ni/SBA-15 catalyst was the most resistant to carbonaceous deposition rationally due to the least NiO crystallite size hindering the nucleation and growth of graphitic carbon. Hence, La-promoted catalyst appeared to be the optimum catalyst in terms of reactant conversion, H_2 yield and stability whilst a gradual decline in both reactant conversion and H_2 yield was experienced with unpromoted and Ce-doped catalysts. Regardless of catalyst types, the ratio of H_2 to CO was always less than unity preferred for Fischer-Tropsch synthesis.

Peer-review under responsibility of the organizing committee of ICPEAM 2016

Keywords: SBA-15; Ni-based catalysts; CeO_2 promoter; La_2O_3 promoter; Syngas; Methane dry reforming

* Corresponding author. Tel.: +6-095-492-874; fax: +6-095-492-889.
E-mail address: vietvo@ump.edu.my

Peer-review under responsibility of the organizing committee of ICPEAM 2016
doi:10.1016/j.proeng.2016.06.556

1. Introduction

Climate change and energy shortage are currently two main global problems. The undesirable rise of anthropogenic greenhouse gas emissions due to the combustion of unsustainable fossil fuels has directly resulted in global warming. The substantial reliance on petroleum-based energy undergoing irrecoverable depletion and the associated release of unfavorable CO_2 gas have prompted campaigns for alternatively clean and renewable energy sources. Syngas regarded as a CO and H_2 mixture has gained significant attention since it can be used as feedstock for Fischer-Tropsch synthesis (FTS) to produce green synthetic fuel and valuable petrochemicals [1, 2]. The conventional and industrial methods for syngas production are steam reforming [3], partial oxidation [4] and autothermal reforming [5] of methane. However, methane dry (or CO_2) reforming (MDR) has been recently recognized as an attractive and efficient process for syngas generation since it involves the conversion of two mainly undesirable greenhouse gases (i.e. CO_2 and CH_4) to useful products [6] and generates syngas with an appropriate H_2/CO ratio for downstream FTS [7-9].

Precious metal-based catalysts reportedly have outstanding coke-resistance, great activity and high selectivity for MDR reaction. They are, however, considerably expensive and low availability [10] and hence unsuitable for industrial application. As a non-noble metal, Ni catalysts supported on various semiconductor oxides, namely, Al_2O_3 [11], TiO_2 [12] and ZrO_2 [11, 13] have been widely investigated for MDR reaction owing to their comparable catalytic performance to noble metals and relatively low price. However, the major constraint associated with Ni-based catalysts is that they are prone to rapid deactivation through sintering of Ni particles due to low Tammann temperature [14] and coking [15, 16] arising from CO disproportionation and CH_4 decomposition reactions as given in Eqs. (1) and (2), respectively.

$$2CO \rightarrow C + CO_2 \quad (\Delta H^0_{298K} = -172.4\ \mathrm{kJ\,mol^{-1}}) \tag{1}$$

$$CH_4 \rightarrow C + 2H_2 \quad (\Delta H^0_{298K} = 75.0\ \mathrm{kJ\,mol^{-1}}) \tag{2}$$

The stability and activity of Ni catalyst for MDR were reportedly enhanced by the impregnation of Ni particles on the mesoporous silica molecular sieve SBA-15 support owing to the possession of high hydrothermal stability, great surface area with ordered mesoporous channels and thick pore walls [17, 18]. However, the knowledge about the promotional effect of lanthanide group on SBA-15 supported Ni catalyst for CO_2 reforming of methane is still limited. Hence, this research aims to examine the role of Ce and La promoters on catalytic stability and activity of Ni/SBA-15 catalysts for MDR reaction. The influence of lanthanide promoters on physicochemical properties was also investigated in this study.

2. Experimental

2.1. Catalyst preparation

In order to synthesize SBA-15 support, approximately 25 g of triblock-poly(ethylene glycol)-block-poly(propylene glycol)-block-poly(ethylene glycol) referred as Pluronic® P-123 ($EO_{20}PO_{70}EO_{20}$ with an average molecular weight of 5800 procured from Sigma-Aldrich Chemicals) was dissolved in 650 mL of HCl solution with controlled pH of about 1 at 303 K. The mixture was subsequently stirred at 1000 rev min^{-1} for 2 h to ensure the complete dissolution of the P-123 triblock copolymer. After dissolving completely surfactant solution, about 50 g of tetraethyl orthosilicate (TEOS from Merck Millipore) was further added dropwise to P-123 mixture and stirred rigorously for 24 h at 310 K. The resulting solid powder was filtered out and washed with deionized water before it was dried at 373 K in an oven followed by calcination in air at 823 K for 6 h with a heating rate of 2 K min^{-1}.

Unpromoted and promoted 10%Ni/SBA-15 catalysts were prepared by incipient wetness impregnation and co-impregnation approaches, respectively. A measured amount of $Ni(NO_3)_2.6H_2O$ and $La(NO_3)_3.6H_2O$ or $Ce(NO_3)_3.6H_2O$ aqueous solutions was impregnated with appropriate amounts of synthesized SBA-15 support to

produce 10%Ni/SBA-15, 3%La-10%Ni/SBA-15 and 3%Ce-10%Ni/SBA-15 catalysts. The mixture was thoroughly stirred in a rotary evaporator (BÜCHI Rotavapor R-200) at 338 K for 2 h under vacuum until water was removed. The solid sample was further dried in an oven for 24 h and calcined with air in the same oven at 973 K for 5 h with a heating rate of 2 K min^{-1}.

2.2. Catalyst characterization

The measurement of Brunauer-Emmett-Teller (BET) surface area for catalysts and associated support was performed in a Micromeritics ASAP-2010 apparatus using N_2 adsorption and desorption isotherms data obtained at 77 K. Prior to each measurement, specimen was outgassed in N_2 flow at 573 K for 1 h to remove moisture and surface contamination. X-ray diffraction (XRD) patterns were measured on a Rigaku Miniflex II system using Cu monochromatic X-ray radiation (with wavelength, $\lambda = 1.5418$ Å) at 30 kV and 15 mA. A relatively small step size of 0.02^0 was used to achieve high resolution during the scanning performed within the range of $2\theta = 3^0$-80^0 at a scan speed of 1^0 min^{-1}. The surface morphology of both the SBA-15 support and Ni-based catalysts was also investigated using a field-emission scanning electron microscope (FESEM) in a JEOL JSM-7800F instrument.

In addition, spent catalysts obtained after MDR reaction were characterized by temperature-programmed oxidation (TPO) in order to determine the types and quantify amounts of deposited carbon formed on catalyst surface during the reforming reaction. About 5 mg of weighed sample mounted in a ceramic crucible was dehydrated at 373 K for 30 min in flowing N_2 of 100 mL min^{-1} before being heated to 1023 K at a ramp rate of 10 K min^{-1} under 100 mL min^{-1} flow of 20%O_2/N_2 mixture. The sample was further kept isothermally at this temperature for 30 min and subsequently cooled down to room temperature in N_2 flow.

2.3. Catalyst testing

The MDR reaction was conducted under atmospheric pressure at 1023 K in a quartz tube fixed-bed continuous flow reactor using about 0.15 g of catalyst mounted in the middle of reactor by quartz wool. The tubular reactor was placed vertically in a split temperature-controlled furnace and reaction temperature was accurately measured with time-on-stream (TOS). The Alicat mass flow controllers were used for regulating precisely the flow rates of CH_4 and CO_2 reactants, which were diluted in N_2 inert gas before directing to the inlet of fixed-bed reactor. The total flow rate of the feed gases (CO_2/CH_4/N_2) was maintained at 60 mL min^{-1} whilst the partial pressure of CO_2 and CH_4 was kept constant at $P_{CO2} = P_{CH4} = 20$ kPa for each run. Catalyst with average particle size of 100-140 μm and gas hourly space velocity (GHSV) of 24 L g_{cat}^{-1} h^{-1} were used for all reactions in order to guarantee negligible mass and heat transport resistances for obtaining the intrinsic catalytic activity. Repeated runs were carried out under the same reaction conditions to confirm the reproducibility of the experimental results. The composition of gaseous product stream from the outlet of fixed-bed reactor was accurately analyzed in a gas chromatograph (Agilent 6890 Series GC system) possessing both FID and TCD detectors.

3. Results and discussion

3.1. Textural properties

The textural properties (including BET surface area, average pore volume and pore diameter) of the promoted and unpromoted catalysts as well as calcined SBA-15 support are summarized in Table 1. The calcined SBA-15 support has a high surface area of about 550 m^2 g^{-1} comparable to other studies [19]. However, a considerable reduction in both BET area and average pore volume was observed with the incorporation of nickel oxide, ceria and lanthana. The inevitable drop in surface area and pore volume indicates the successful diffusion of both active metal and promoter to the ordered mesoporous channels of SBA-15 support. Additionally, pore blockage due to the agglomeration of NiO particles on pore entrances could induce a decline in these textural attributes.

Table 1. Summary of physical properties for SBA-15 support, promoted and unpromoted Ni-based catalysts.

Catalysts	BET surface area ($m^2 g^{-1}$)	Average pore volume [a] ($cm^3 g^{-1}$)	Average pore diameter (nm)	Average crystallite size [b] (nm)
Calcined SBA-15 support	550.05 ± 9.83	0.49	3.59	-
10%Ni/SBA-15	444.96 ± 6.57	0.40	3.61	27.04
3%La-10%Ni/SBA-15	303.24 ± 3.29	0.33	4.43	19.09
3%Ce-10%Ni/SBA-15	348.21 ± 5.11	0.31	3.87	20.28

[a] Calculation was based on Barret-Joyner-Halenda (BJH) desorption method.

[b] Average crystallite size was estimated from XRD pattern using Scherrer equation [20].

3.2. X-ray diffraction measurement

Fig. 1 shows the XRD patterns of fresh mesoporous SBA-15 support, unpromoted and promoted 10%Ni/SBA-15 catalysts. X-ray diffractograms were interpreted using the Joint Committee on Powder Diffraction Standards (JCPDS) database [21]. The broad peak located at about $2\theta = 15^0 – 30^0$ (cf. Figs. 1(a)-(d)) is ascribed to the SiO_2 frameworks of the SBA-15 support (JCPDS card No. 29-0085) for all samples in agreement with other studies [18, 22]. The characteristic peaks of crystalline NiO phase (JCPDS card No. 47-1049) were also detected at $2\theta = 37.3^0$, 43.3^0, 63.0^0 and 75.5^0 for both promoted and unpromoted catalysts. However, there were no visible peaks for La_2O_3 and CeO_2 phases in the XRD patterns of the promoted catalysts, suggesting that both La and Ce promoters were highly dispersed on the surface of Ni/SBA-15 catalyst reasonably due to the great BET surface area of the mesoporous SBA-15 support as seen in Table 1. Interestingly, as seen in Table 1, the average crystallite size of NiO particles was reduced from 27.0 to 20.3 or 19.1 nm with the corresponding Ce or La addition indicating the increasing metal dispersion. This could be due to the strong interaction between promoter and NiO particles preventing the aggregation of NiO crystallites.

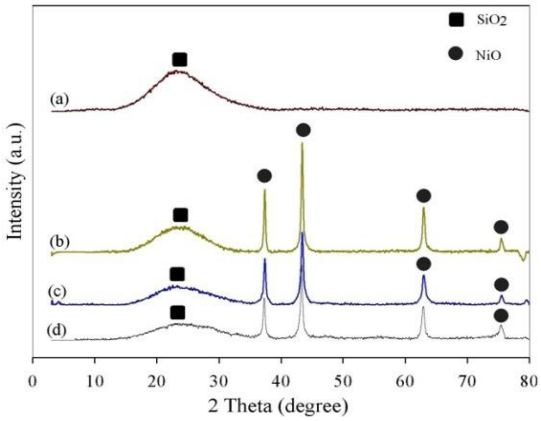

Fig. 1. XRD patterns of (a) SBA-15 support, (b) 10%Ni/SBA-15, (c) 3%La-10%Ni/SBA-15 and (d) 3%Ce-10%Ni/SBA-15 catalysts.

3.3. Field-emission scanning electron microscope analysis

The FESEM measurement was performed in order to study the surface morphology of the SBA-15 support, doped and undoped Ni/SBA-15 catalysts as shown in Fig. 2. FESEM micrograph displays that SBA-15 particles possess a fairly uniform rod-like shape with a diameter of about 0.55 µm (cf. Fig. 2(a)). These particles seemed to gather to form wheat-like microstructures with ordered mesoporous channels consistent with other reports [23, 24]. As illustrated in Figs. 2(b)-(d), NiO particles also aggregated on the support surface leading to a considerable decrease in BET surface area (cf. Table 1).

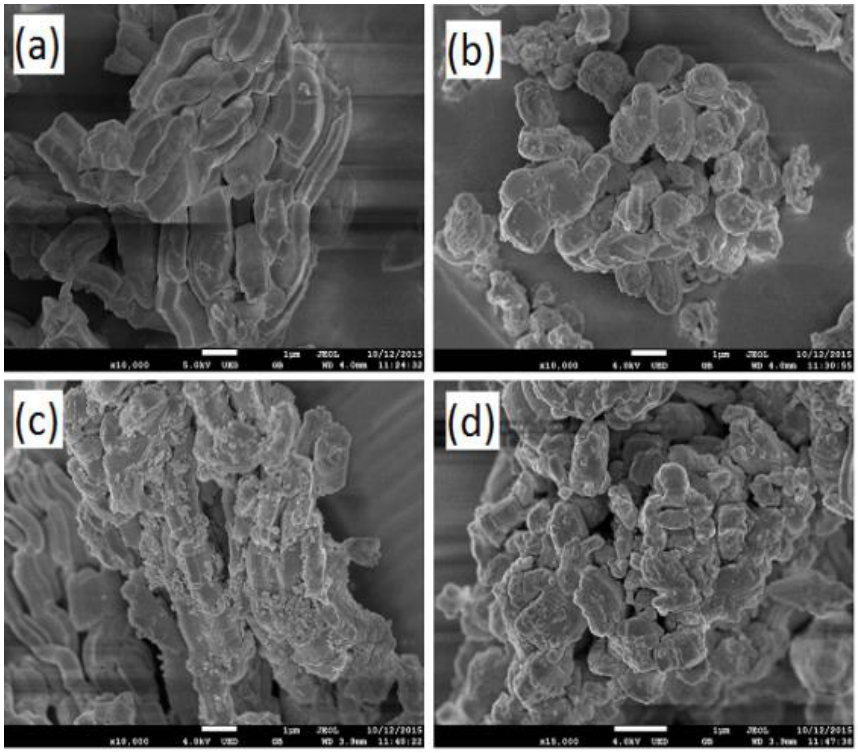

Fig. 2. FESEM images of (a) mesoporous SBA-15, (b) unpromoted 10%Ni/SBA-15, (c) promoted 3%La-10%Ni/SBA-15, and (d) promoted 3%Ce-10%Ni/SBA-15 before CRM reaction.

3.4. Temperature-programmed oxidation

The TPO measurements of spent catalysts collected after MDR reaction for 24 h at 1023 K and $P_{CO2} = P_{CH4} = 20$ kPa were also conducted to estimate the amount of carbonaceous deposition. Fig. 3 represents the TPO profiles of spent unpromoted and promoted Ni/SBA-15 catalysts. A high intensity peak located at high oxidation temperature ranging from 750-970 K for each catalyst was assigned to the gasification of graphitic carbon [25, 26]. The integrated peak area decreased in the order; unpromoted 10%Ni/SBA-15 > Ce-promoted > La-promoted catalysts suggesting the increasing carbon resistance with promoter modification. However, the similar temperature range of oxidation peaks for all spent catalysts indicated that the analogous type of carbon was formed during MDR reaction and the structure of deposited carbon was not significantly affected by Ce and La promoters. The enhancement of carbon resilience with promoter addition was reasonably due to the basic property of CeO_2 and La_2O_3 dopants improving CO_2 chemisorption and hence increasing the reverse-Boudouard reaction for carbon elimination [27]. In addition, the excellent oxygen storage-release capacity of these promoters could be responsible for the less carbon deposition rate observed [28]. In fact, the mobile oxygen released from the lattice of promoters could simultaneously gasify the carbonaceous deposition and keep the active sites of catalysts free from deposited carbon whilst the oxygen vacancies could be refilled by CO_2 oxidation [18, 28]. Additionally, as seen in Fig. 3, La-promoted catalyst was more resistant to carbon deposition than Ce-doped catalyst since La-promoted catalyst possessed a smaller NiO crystallite size (cf. Table 1). Christensen *et al*. reported that lesser size of NiO crystals had a greater saturation concentration of carbon and hence a lower driving force for diffusing carbon through NiO particles [29].

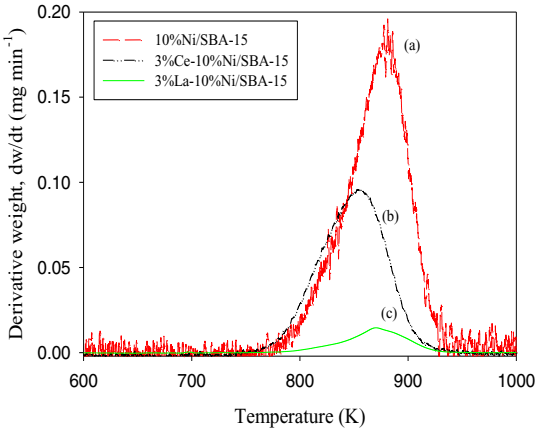

Fig. 3. Derivative weight profiles for temperature-programmed oxidation of spent catalysts including (a) 10%Ni/SBA-15, (b) 3%Ce-10%Ni/SBA-15 and (c) 3%La-10%Ni/SBA-15 catalysts after 24 h on-stream at temperature of 1023 K and $P_{CO2} = P_{CH4} = 20$ kPa.

3.5. Catalytic activity and stability

A long-term stability test of 24 h was performed for both promoted and unpromoted 10%Ni/SBA-15 catalysts in order to examine catalytic performance and stability for MDR reaction. As seen in Fig. 4, both CH_4 and CO_2 conversions improved with promoter addition in the order; unpromoted < Ce-promoted < La-promoted 10%Ni/SBA-15 catalysts opposite to the trend of carbon deposition (cf. Fig. 3) responsible for low catalytic activity and high deactivation. CH_4 and CO_2 conversions of unpromoted and Ce-doped catalysts decreased gradually with time-on-stream whilst La-promoted catalyst appeared to be stable over a period of 24 h on-stream rationally owing to the lowest carbon deposition associated with the smallest NiO crystallite size unfavorable for carbon formation [27, 29], the basic character [27] and high oxygen storage capacity of La_2O_3 promoter [18, 28] gasifying deposited carbon from methane decomposition reaction. Interestingly, regardless of doped and undoped catalysts, the conversion of CO_2 was always superior to that of CH_4 symptomatic of the presence of concomitant reverse water-gas shift (RWGS) reaction. In fact, H_2/CO values of all catalysts were less than the stoichiometric ratio of 1 further confirming the coexistence of RWGS reaction (cf. Fig. 5(a)). Remarkably, La-promoted catalyst also exhibited the highest H_2 yield of about 80% followed by Ce-doped and undoped catalysts as seen in Fig. 5(b).

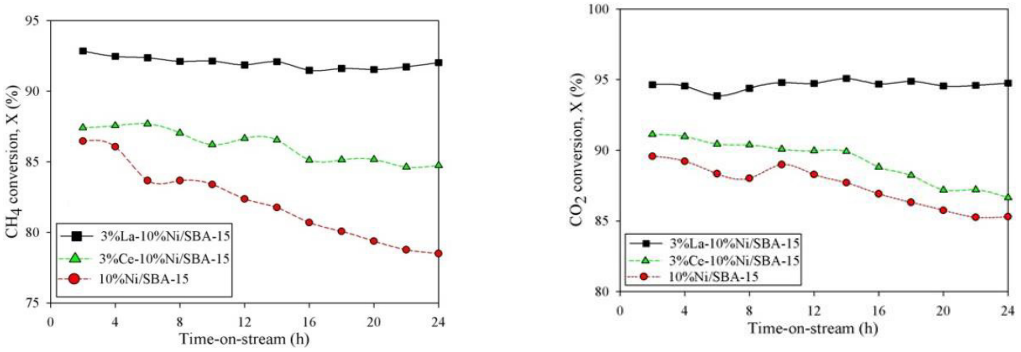

(a) (b)

Fig. 4. Effect of promoter on (a) CH_4 and (b) CO_2 conversions with time-on-stream at $P_{CO2} = P_{CH4} = 20$ kPa and 1023 K.

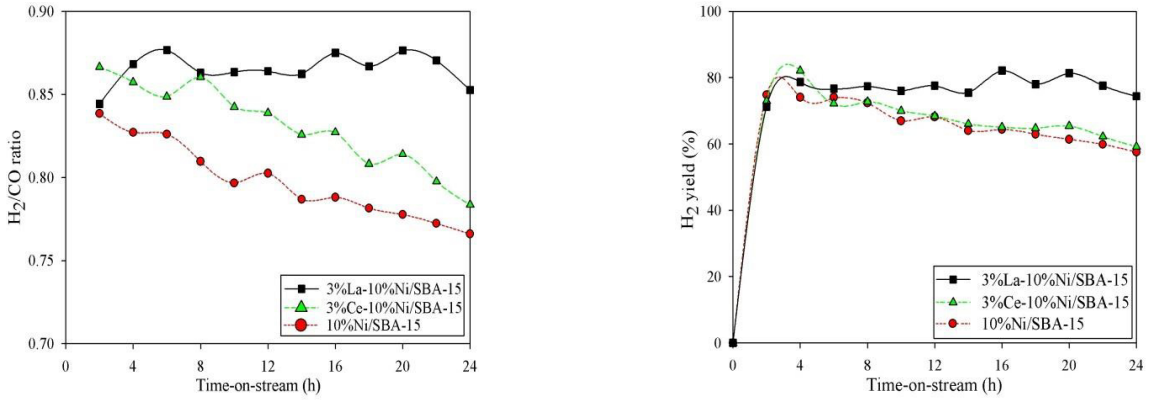

Fig. 5. Effect of promoter on (a) H_2/CO ratio and (b) H_2 yield with time-on-stream at $P_{CO2} = P_{CH4} = 20$ kPa and 1023 K.

4. Conclusion

La- and Ce-promoted 10%Ni/SBA-15 catalysts have been successfully synthesized by the incipient wetness impregnation method. Promoted and unpromoted catalysts exhibited high BET surface area ranging from 303-445 $m^2\ g^{-1}$. Both active metal and promoters were effectively diffused into the ordered mesoporous channels of SBA-15 support. The crystallite size of NiO phase was reduced with promoter addition from 27.0 to 19.1 nm and promoters were finely dispersed on the catalyst surface. The TPO measurements showed that the promotion of La_2O_3 and CeO_2 improved carbon resilience and La-doped catalyst possessed the highest resistance to coking because of its smallest NiO crystallite size preventing the nucleation and growth of carbonaceous deposition. Apart from La-promoted catalyst, Ce-doped and undoped 10%Ni/SBA-15 catalysts experienced a gradual decline in reactant conversion and H_2 yield. La-promoted catalyst seemed to be the optimal catalyst in terms of conversion, H_2 yield and stability. H_2/CO ratio of less than unity for both unpromoted and promoted catalysts indicated the occurrence of a parallel side reaction, i.e., RWGS reaction consuming H_2 to form more CO gaseous product.

Acknowledgements

The authors are grateful for the financial support from UMP Research Grant Scheme (RDU140374) to conduct this study.

References

[1] G.L. Bezemer, J.H. Bitter, H.P.C.E. Kuipers, H. Oosterbeek, J.E. Holewijn, X. Xu, F. Kapteijn, A.J.V. Dillen, K.P. De Jong, Cobalt Particle Size Effects in the Fischer-Tropsch Reaction Studied with Carbon Nanofiber Supported Catalysts, J. Am. Chem. Soc. 128 (2006) 3956-3964.
[2] D.-V.N. Vo, V. Arcotumapathy, B. Abdullah, A.A. Adesina, Evaluation of Ba-promoted Mo carbide catalyst for Fischer-Tropsch synthesis, J. Chem. Technol. Biotechnol. 88 (2013) 1358-1363.
[3] V. Arcotumapathy, D.-V.N. Vo, D. Chesterfield, C.T. Tin, A. Siahvashi, F.P. Lucien, A.A. Adesina, Catalyst design for methane steam reforming, Appl. Catal. A: Gen. 479 (2014) 87-102.
[4] Y. Kobayashi, J. Horiguchi, S. Kobayashi, Y. Yamazaki, K. Omata, D. Nagao, M. Konno, M. Yamada, Effect of NiO content in mesoporous NiO-Al_2O_3 catalysts for high pressure partial oxidation of methane to syngas, Appl. Catal. A: Gen. 395 (2011) 129–137.
[5] S. Ayabe, H. Omoto, T. Utaka, R. Kikuchi, K. Sasaki, Y. Teraoka, K. Eguchi, Catalytic autothermal reforming of methane and propane over supported metal catalysts, Appl. Catal. A: Gen. 241 (2003) 261–269.
[6] M.E. Gálvez, A. Albarazi, P. Da Costa, Enhanced catalytic stability through non-conventional synthesis of Ni/SBA-15 for methane dry reforming at low temperatures, Appl. Catal. A: Gen. 504 (2015) 143–150.
[7] M. Yu, Y.A. Zhu, Y. Lu, G. Tong, K. Zhu, X. Zhou, The promoting role of Ag in Ni-CeO_2 catalyzed CH_4-CO_2 dry reforming reaction, Appl. Catal. B: Environ. 165 (2015) 43–56.

[8] I. Rivas, J. Alvarez, E. Pietri, M.J. Pérez-Zurita, M.R. Goldwasser, Perovskite-type oxides in methane dry reforming: Effect of their incorporation into a mesoporous SBA-15 silica-host, Catal. Today 149 (2010) 388-393.
[9] N. Wang, X. Yu, K. Shen, W. Chu, W. Qian, Synthesis, characterization and catalytic performance of MgO-coated Ni/SBA-15 catalysts for methane dry reforming to syngas and hydrogen, Int. J. Hydrogen Energy 38 (2013) 9718-9731.
[10] K. Jabbour, N. El Hassan, S. Casale, J. Estephane, H. El Zakhem, Promotional effect of Ru on the activity and stability of Co/SBA-15 catalysts in dry reforming of methane, Int. J. Hydrogen Energy 39 (2014) 7780-7787.
[11] F. Pompeo, N.N. Nichio, M.M.V.M. Souza, D. V. Cesar, O. A. Ferretti, M. Schmal, Study of Ni and Pt catalysts supported on α-Al_2O_3 and ZrO_2 applied in methane reforming with CO_2, Appl. Catal. A: Gen. 316 (2007) 175-183.
[12] S.S. Kim, S.M. Lee, J.M. Won, H.J. Yang, S.C. Hong, Effect of Ce/Ti ratio on the catalytic activity and stability of Ni/CeO_2–TiO_2 catalyst for dry reforming of methane, Chem. Eng. J. 280 (2015) 433-440.
[13] M. Németh, Z. Schay, D. Srankó, J. Károlyi, G. Sáfrán, I. Sajó, A. Horváth, Impregnated Ni/ZrO_2 and Pt/ZrO_2 catalysts in dry reforming of methane: Activity tests in excess methane and mechanistic studies with labeled $^{13}CO_2$, Appl. Catal. A: Gen. 504 (2015) 608-620.
[14] L. Xu, H. Song, L. Chou, One-Pot Synthesis of Ordered Mesoporous NiO–CaO–Al_2O_3 Composite Oxides for Catalyzing CO_2 Reforming of CH_4, ACS Catal. 2 (2012) 1331-1342.
[15] M.H. Amin, K. Mantri, J. Newnham, J. Tardio, S.K. Bhargava, Highly stable ytterbium promoted Ni/γ- Al_2O_3 catalysts for carbon dioxide reforming of methane, Appl. Catal. B Environ. 119-120 (2012) 217–226.
[16] J. Newnham, K. Mantri, M.H. Amin, J. Tardio, S.K. Bhargava, Highly stable and active Ni-mesoporous alumina catalysts for dry reforming of methane, Int. J. Hydrogen Energy 37 (2012) 1454–1464.
[17] G. Du, S. Lim, M. Pinault, C. Wang, F. Fang, L. Pfefferle, G. L. Haller, Synthesis, characterization, and catalytic performance of highly dispersed vanadium grafted SBA-15 catalyst, J. Catal. 253 (2008) 74–90.
[18] D. Li, L. Zeng, X. Li, X. Wang, H. Ma, S. Assabumrungrat, J. Gong, Ceria-promoted Ni/SBA-15 catalysts for ethanol steam reforming with enhanced activity and resistance to deactivation, Appl. Catal. B: Environ. 176–177 (2015) 532-541.
[19] H. Zhang, M. Li, P. Xiao, D. Liu, C.-J. Zou, Structure and Catalytic Performance of Mg-SBA-15-supported Nickel Catalysts for CO_2 Reforming of Methane to Syngas, Chem. Eng. Technol. 36 (2013) 1701-1707.
[20] A.L. Patterson, The Scherrer formula for X-ray particle size determination, Phys. Rev. 56 (1939) 978-982.
[21] JCPDS Powder Diffraction File. International Centre for Diffraction Data. Swarthmore, PA; 2000.
[22] H. Liu, H. Wang, J. Shen, Y. Sun, Z. Liu, Promotion effect of cerium and lanthanum oxides on Ni/SBA-15 catalyst for ammonia decomposition, Catal. Today, 131 (2008) 444–449.
[23] Y. Li, N. Sun, L. Li, N. Zhao, F. Xiao, W. Wei, Y. Sun, Grafting of amines on ethanol-extracted SBA-15 for CO_2 adsorption, Materials 6 (2013) 981–999.
[24] P. Shukla, H. Sun, S. Wang, H.M. Ang, M.O. Tadé, Co-SBA-15 for heterogeneous oxidation of phenol with sulfate radical for wastewater treatment, Catal. Today 175 (2011) 380–385.
[25] C.H. Bartholomew, Mechanisms of catalyst deactivation. Appl. Catal. A: Gen. 212 (2001) 17–60.
[26] K. Selvarajah, N.H.H. Phuc, B. Abdullah, F. Alenazey, D.-V.N. Vo, Syngas production from methane dry reforming over Ni/Al_2O_3 catalyst, Res. Chem. Intermed. 42 (2016) 269–288.
[27] R. Yang, C. Xing, C. Lv, L. Shi, N. Tsubaki, Promotional effect of La_2O_3 and CeO_2 on Ni/γ-Al_2O_3 catalysts for CO_2 reforming of CH_4, Appl. Catal. A: Gen. 385 (2010) 92–100.
[28] S.Y. Foo, C.K. Cheng, T.H. Nguyen, A.A. Adesina, Evaluation of lanthanide-group promoters on Co-Ni/Al_2O_3 catalysts for CH_4 dry reforming, J. Mol. Catal. A: Chem. 344 (2011) 28–36.
[29] K.O. Christensen, D. Chen, R. Lødeng, A. Holmen, Effect of supports and Ni crystal size on carbon formation and sintering during steam methane reforming, Appl. Catal. A: Gen. 314 (2006) 9–22.